Establishing the ground-state spin of math xmlns="http://www.w3.org/1998/Math/MathML">mmultiscripts>mi>Kr/mi>mprescripts>/mprescripts>none>/none>mn>71/mn>/mmultiscripts>/math>

S. Waniganeththi, D. E. M. Hoff, A. M. Rogers, C. J. Lister, P. C. Bender, K. Brandenburg, K. Childers, J. A. Clark, A. C. Dombos, E. R. Doucet, S. Jin, R. Lewis, S. N. Liddick, Z. Meisel, C. Morse, H. Schatz, K. Schmidt, D. Soltesz, and S. K. Subedi

Phys. Rev. C **106**, 044317 — Published 17 October 2022

DOI: 10.1103/PhysRevC.106.044317

Establishing the ground-state spin of ^{71}Kr

S. Waniganeththi,[1,*] D. E. M. Hoff,[1,2] A. M. Rogers,[1,†] C. J. Lister,[1] P. C. Bender,[1] K. Brandenburg,[3] K. Childers,[4,5] J. A. Clark,[6] A. C. Dombos,[4,7,8] E. R. Doucet,[1] S. Jin,[4,7,8] R. Lewis,[4,5] S. N. Liddick,[4,5] Z. Meisel,[3] C. Morse,[1,9] H. Schatz,[4,7,8] K. Schmidt,[4,8,‡] D. Soltesz,[3] and S. K. Subedi[3]

[1]*Department of Physics and Applied Physics, University of Massachusetts Lowell, Lowell, MA 01854*
[2]*Lawrence Livermore National Laboratory, Livermore, CA 94550*
[3]*Institute of Nuclear and Particle Physics, Department of Physics and Astronomy, Ohio University, Athens, OH 45701*
[4]*National Superconducting Cyclotron Laboratory, Michigan State University, East Lansing, MI 48824*
[5]*Department of Chemistry, Michigan State University, East Lansing, Michigan 48824*
[6]*Physics Division, Argonne National Laboratory, Argonne, IL 60439*
[7]*Department of Physics and Astronomy, Michigan State University, East Lansing, Michigan 48824*
[8]*JINA-CEE, Michigan State University, East Lansing, MI 48824*
[9]*National Nuclear Data Center, Brookhaven National Laboratory, Upton, New York 11973*

(Dated: October 4, 2022)

Nuclei in the vicinity of the $N = Z$ line provide many sensitive probes of isospin symmetry. One example concerns the character and sequence of low-lying states of the $T = 1/2$ mirror pair ^{71}Kr and ^{71}Br which has been under debate for several decades. In this paper we report a new measurement of the absolute β-branching to ground and excited states which, taken with our precise lifetime of $T_{1/2} = 94.9(4)$ ms, gives a super allowed ground state-to-ground state $\log(ft)$ value of 3.64(4). This is only consistent with both ^{71}Br and ^{71}Kr having the same spin and parity, $J^\pi = 5/2^-$, as expected from mirror symmetry. The β-delayed proton emission to the first-excited state in ^{70}Se was observed for the first time which also strongly supports this assignment.

I. INTRODUCTION

Isospin symmetry is only an approximate symmetry of the nuclear Hamiltonian due to the presence of electromagnetic interactions, isospin non-conserving components of the strong force, and differences between the neutron and proton masses [1–4]. Nonetheless this symmetry, while imperfect, is a tool which allows all nuclear states to be characterized by the isospin quantum number, T, emphasizing the underlying charge symmetry and charge independence of the strong nuclear two-body interaction [5]. Mirror nuclei are ideal systems for probing isospin symmetry as their structure should be nearly identical, particularly their ground states [6, 7].

The largest source of isospin-symmetry breaking is generated by the Coulomb interaction which becomes increasingly significant for the higher-mass members of isospin multiplets along the $N = Z$ line. Studying these neutron-deficient higher mass systems is challenging, however, as the $N = Z$ line lies farther from stability with increasing mass and the relevant nuclei become weakly bound or even unbound in their ground state.

In the *fpg* shell-model space, shape coexistence is a well-known phenomenon that adds another layer of complexity to understanding nuclear structure and symmetries. In the $A \approx 70$ mass region oblate-prolate shape coexistence is well known [8, 9] and of significant interest [10–14]. It remains an open question as to whether the variation of the Coulomb energy associated with different shapes can cause a reordering of levels and a significant change in the structure of mirror partners. The focus of this work is to address the symmetry between the mirror pair $^{71}_{36}$Kr$_{35}$ and $^{71}_{35}$Br$_{36}$ and to better understand the underlying nuclear structure. The character of the ^{71}Kr ground state, specifically its spin and parity assignment, has been under debate for many years.

^{71}Kr exhibits decay through β-delayed proton emission [15–17]. Detailed β-decay spectroscopy on ^{71}Kr was performed at ISOLDE [18] where ^{71}Kr ions were produced through spallation reactions in a Nb foil using a 1-GeV proton beam and implanted onto a tape for study. Normally, for $T = 1/2$ pairs, the decay is dominantly ground state-to-ground state, as the wave functions are nearly identical except for the exchange of a proton for a neutron. In this case, however, a significant population of excited states was observed. A reinterpretation of Ref. [18] was proposed by Urkedal and Hamamoto [19] in which they suggested that the ground-state spins of this mirror pair differed, and thus the normal decay pattern was disrupted. Fischer et al. [20] then performed an in-beam spectroscopic measurement of ^{71}Br using Gammasphere to explore the question of the ground-state spin of ^{71}Kr. Based on the detailed level scheme deduced by Fischer et al., and the assignment of spins and parities allowing the band structure to be clarified, an altered β-decay scheme for ^{71}Kr was proposed. In particular, the ground-state of ^{71}Br was constrained to have a J^π of $5/2^-$ and the low-lying 10-keV state in ^{71}Br was assigned $1/2^-$. The analysis supported the notion that ^{71}Kr had a ground-state J^π of $5/2^-$, in accordance with mirror symmetry, but inferred an even larger excited-state population in the ^{71}Kr$\rightarrow$ ^{71}Br decay, which was highly anomalous and

* email:Sanjanee_Waniganeththi@student.uml.edu
† email:Andrew_Rogers@uml.edu
‡ Present Address: *Institute of Radiation Physics, Helmholtz-Zentrum Dresden-Rossendorf, Dresden, Germany 01328*

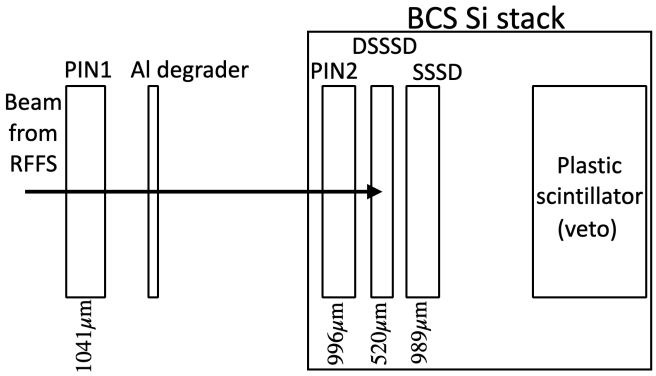

FIG. 1. Schematic representation of the Si detectors comprising the NSCL β-Counting System in the configuration used for this experiment. The degrader was adjusted to ensure implantation within the DSSSD. The implantation stack was surrounded by the Segmented Germanium Array (not shown) to detect coincident γ-rays. Distances and dimensions are not to scale.

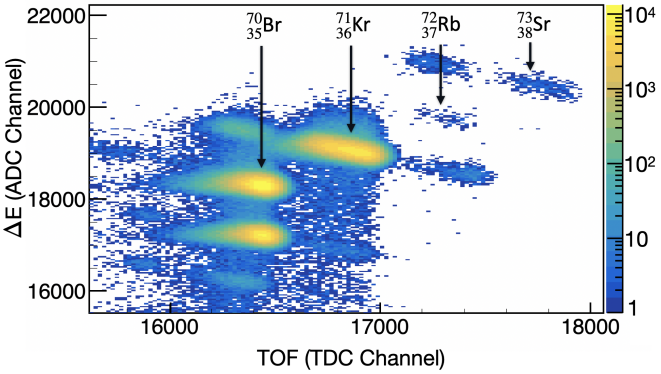

FIG. 2. Particle identification plot of implanted ions with well-defined implantation signals and plastic-scintillator veto. The PID plot shows the PIN1 (ΔE) measurement versus the TOF measured between PIN2 and the A1900 Focal Plane scintillator.

inconsistent with all other well-studied $T = 1/2$ mirror decays.

Here we seek to clarify this problem by studying in more detail the β decay of ^{71}Kr to excited states in ^{71}Br and, via β-delayed proton emission, to states in ^{70}Se.

II. EXPERIMENT

Neutron-deficient nuclei in this study were produced by projectile fragmentation of a 140-MeV/nucleon ^{92}Mo beam, accelerated by the Coupled Cyclotron Facility (CCF) at the National Superconducting Cyclotron Laboratory (NSCL), and impinged upon a 152.2-mg/cm^2 Be target. The beam was analyzed by passing the ions through the A1900 fragment separator [21] and further purified using the Radio Frequency Fragment Separator (RFFS) [22]. Over the course of the experiment, the ^{71}Kr implantation rate was 2 ions/sec and the total implantation rate was about 10 ions/sec. The secondary cocktail beam was implanted into the β-counting station (BCS) [23] comprised of a detector stack, as indicated in Fig. 1, and surrounded by the Segmented Germanium Array (SeGA) [24]. As part of the BCS, a 1041-μm thick silicon PIN detector (PIN1) and a variable-thickness Al degrader were placed about 1-m upstream from the implantation stack. The stack consisted of a 996-μm thick silicon PIN detector (PIN2) followed by a 520-μm thick 40-mm$\times$40-mm Double-Sided Silicon-Strip Detector (DSSSD) used as the implantation detector. The DSSSD was segmented into 40x40, 1-mm perpendicular front and back strips, defining a total of 1600 pixels. This was followed by a 989-μm thick 16-strip Single-Sided Silicon Strip Detector (SSSD). At the end of the stack, a plastic scintillator was used to veto events corresponding to ions that passed through the silicon stack.

Each implanted ion was identified based on the measured energy loss (ΔE) and Time-Of-Flight (TOF). TOF information was determined from the time difference between the start signal provided by PIN2 and a stop signal given by a scintillator located at the extended focal plane (XFP) of the A1900. To improve the identification, any ions that did not generate a well-defined implantation signal in a pixel or ions detected in the plastic scintillator (ions that passed through the implantation detector), were vetoed from the particle identification (PID). This process was also useful in removing fragments that underwent secondary reactions. The resulting particle identification spectrum for the region of interest is shown in Fig. 2. Ion identification was confirmed by the observation of known γ rays.

All of the detector signals were collected using a digital data acquisition system that utilized XIA Pixie-16 digitizers with 250-MHz ADCs and 100-MHz clocks [25]. Apart from pulse-height and timing data, waveforms of the DSSSD signals were acquired for offline analysis.

During a typical implantation event several GeV of energy is deposited into the DSSSD. Decay events, however, generate a significantly lower amount of energy, on the order of MeV or less. Therefore, to cover the full energy range in the DSSSD, dual-gain pre-amplifiers were used that contained a low-gain stage for the implantation signals and a high-gain stage for the lower-energy decay signals [23]. The strips with the largest signal were used to identify the implantation pixel. A high-gain pre-amplifier output in both front and back channels with no PIN1 signal is defined as a potential decay event. Event selection required that a decay occurred within a defined time window based on the half-life of the ion of interest and that the decay event occurred in the same pixel or nearest surrounding 24-pixels relative to the implantation event.

SeGA was employed to detect both the prompt and β-delayed γ rays after the implantation event. The array consisted of a total of 16 high-purity germanium detectors. In the offline data analysis, γ-ray signals were correlated up to 5 μs after a potential decay event.

The DSSSD high-gain channels were energy calibrated with ^{228}Th and ^{148}Gd α sources, with corrections for a 0.1-nm Al dead layer on the front of the detector. The energy and absolute efficiency calibrations for SeGA were performed with a ^{60}Co source and a Standard Reference Material (SRM) containing ^{125}Sb, ^{125m}Te, ^{154}Eu, and ^{155}Eu.

III. EXPERIMENTAL RESULTS

A. ^{71}Kr half-life measurement

The time distribution of decay events correlated within a 5-s time window of implanted and identified ^{71}Kr ions is shown in Fig. 3 for correlation times up to 1.5 s. The β-decay daughter (^{71}Br) and proton-decay daughter (^{70}Se) have half-lives of 21.4(6) s [26] and 41.1(3) min [27, 28], respectively, that are significantly longer than the correlation window. A simple parent decay law with a constant background was found to provide a satisfactory fit to the data. The half-life was determined by a reduced χ^2-minimization fit, which provided a value of 94.9(4) ms for ^{71}Kr where the uncertainty includes both statistical ($\pm$0.34 ms) and systematic ($\pm$0.11 ms) contributions combined in quadrature. The systematic uncertainty was estimated by varying the binning as well as the beginning and end of the fit range. Gating on the 198/199 keV γ-ray transition in the ^{71}Br daughter (discussed in the next section) a half-life of 95.3(22) ms was found which is in excellent agreement, although with a larger uncertainty due to the reduction in statistics using this method. Consequently, we adopt the higher precision half-life of 94.9(4) ms for ^{71}Kr. This measured half-life is in disagreement with both the current evaluated ENSDF value of 100(3) ms [18] and a more recent as well as more precise unevaluated value of 98.8(3) ms reported in Ref. [29].

B. γ-ray spectroscopy

To remove background due to random coincidences in the β-gated γ-ray spectra, the correlation time was limited to 1 s and the scaled γ-ray background, obtained from β-gated γ-ray correlations in the 1-5 s correlation time interval where the background is constant, was subtracted. Figure 4 shows this subtracted spectrum and highlights the relevant γ-ray transitions in this work.

Transition energies of 198/199, 208, 397, and 407 keV are observed and are attributed to the de-excitation of the low-lying negative parity levels of ^{71}Br based on the established level and γ-decay scheme of Fischer et al. [20]. Events correlated with 198/199-keV γ rays were used to cleanly select and verify the measured ^{71}Kr half-life. No evidence was found for population of positive parity states nor was there clear evidence for additional transitions.

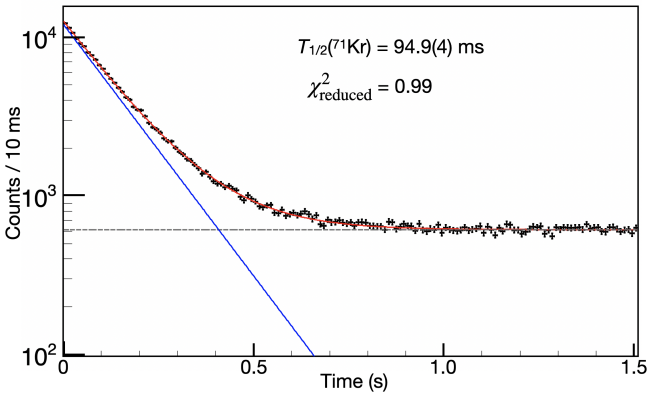

FIG. 3. Time distribution of decay events following the implantation of ^{71}Kr nuclei. The decay-time spectrum was fit over the full correlation window of 5 s with an exponential function (solid blue) together with a constant background (dashed gray) resulting in the combined fit (solid red). The half-life extracted for ^{71}Kr is $T_{1/2}$=94.9(4) ms where the uncertainty is composed of the statistical and systematic error added in quadrature.

Determining γ-ray transition intensities associated with the ^{71}Kr decay was complicated by the fact that the 198/199-, 208-, and 407-keV transitions in ^{71}Br are degenerate, as found in the level scheme devised by Fischer et al. [20]. Specifically, γ-ray transitions with energies of 208- and 407-keV are produced through direct depopulation of the 208- and 407-keV levels to the ground state as well as through depopulating the 615-keV state to the 407- and 208-keV levels. The de-excitation of the 407-keV state to the 208-keV state followed by a transition to the 10-keV level produces coincident 199- and 198-keV γ rays, respectively, and is observed as a doublet in our spectra.

$\gamma\gamma$ coincidences were used to disentangle which levels are populated in the β decay and, together with the efficiencies to be discussed in Sec. IV E, transition and β^+/EC intensities were determined. The panels in Fig. 5 show the relevant delayed $\gamma\gamma$ coincidence spectra. Figure 5(a) shows the result of a gate on the 198/199-keV photopeak, indicating that the 198/199-keV transitions are in self coincidence. Together with the 397- and 407-keV lines, this indicates β feeding to the 407-keV level. Furthermore, there is little evidence in either Fig. 5(a) or (b) for coincidence with a 407-keV line which would indicate population of the 615-keV level in ^{71}Br. Consequently, the analysis presented here assumes that there is negligible feeding to states above the 407-keV level. Even so, these observations appear to be in agreement with the low-lying ^{71}Br de-excitation scheme published by Fischer et al. [20]. Under these assumptions, the absolute intensity of the 199-keV transition is calculated as the sum of the coincident 198/199 $\gamma\gamma$ intensity and the 199-keV intensity as determined from a coincidence gate on the 208-keV γ-ray. The absolute intensity of the 198-keV transition is determined by subtracting the 199-keV

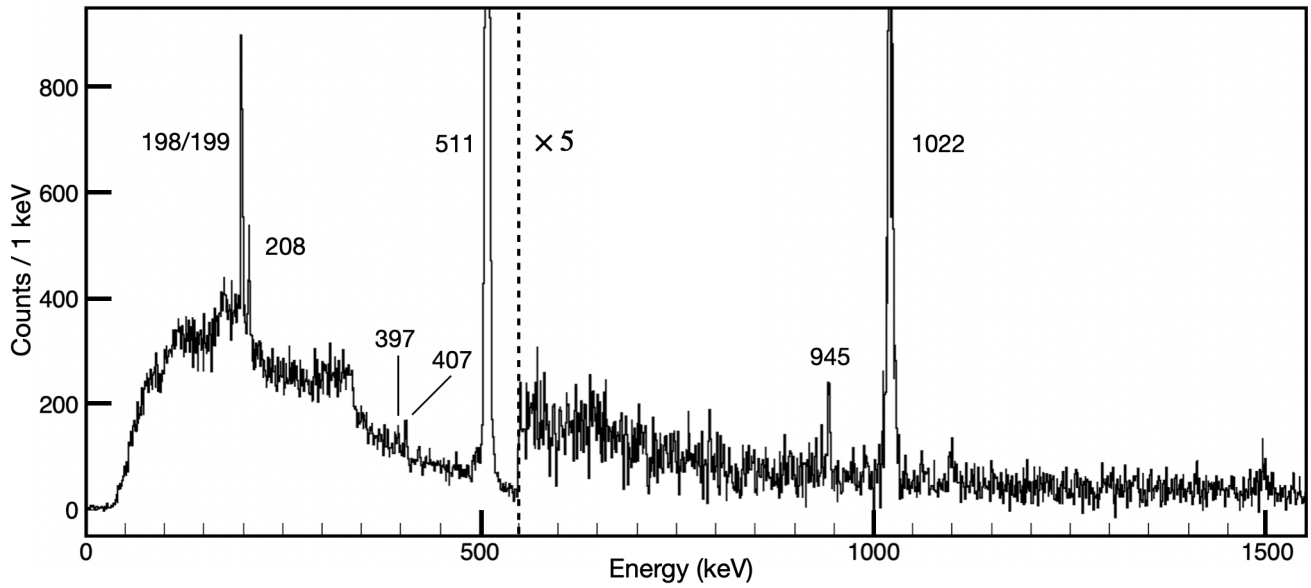

FIG. 4. Background-subtracted ^{71}Kr γ-ray spectrum. To produce this spectrum, β-gated γ rays were correlated up to 1 s after implantation. A time normalized β-gated γ-spectrum was also generated for γ rays correlated between 1-5 seconds after implantation. The residual subtracted spectrum is shown with indicated transitions corresponding to the de-excitation of ^{71}Br observed at energies of 198/199, 207, 397 and 407 keV. For clarity, the scale above 550 keV has been increased by a factor of 5. This expanded energy region shows the $2^+ \rightarrow 0^+$ 945-keV transition in ^{70}Se along with a peak at 1022 keV due to 511-keV summation.

intensity from the intensity of the 198/199-keV doublet. Because of the ambiguity in the overlapping transitions, quantitative comparison to the results of Fisher et al. [20] was challenging and is discussed in Sec. V.

C. Charged-particle spectroscopy

β-delayed proton spectroscopy was performed by using the energy deposited in the DSSSD for the correlated decay events. While protons are mostly stopped and deposit their full energy in most cases, β particles will deposit only a small fraction of their energy. For β-delayed proton events, the detected energy will be the sum of the proton energy and the partial energy deposition from the positron.

The time correlated background subtraction was performed following the same procedure that was used for the γ-ray energy spectrum. The similarity of the shape of the background charged-particle spectrum (red) in Fig. 6 to the true correlated spectrum (blue) is due predominately to other implanted ^{71}Kr ions, as they are the strongest group implanted into the detector. The background subtracted charged-particle spectrum of ^{71}Kr β-delayed proton-emission events is shown in black in Fig. 6. In the energy range of 1.5 to 5.0 MeV, several broad features are observed associated with β-delayed proton decay events. These structures arise from the decay of the continuum of levels populated in ^{71}Br that lie above the proton separation energy (S_p = 1861(6) keV [30]) and result in ^{70}Se production. According to Fig. 7 these features are in coincidence with 511- and 945-keV γ rays. The 945-keV γ ray corresponds to the de-excitation from the first-excited (2^+) state of ^{70}Se to its ground state.

IV. ANALYSIS

A. The decay scheme

The decay scheme of ^{71}Kr deduced from the results of the present experiment together with the identified γ-ray transition energies from Ref. [20], is shown in Fig. 8. The energies of the γ rays and the total transition intensities, $I_{\gamma+\mathrm{ce}}$, are given which include a correction for internal conversion assuming pure M1 transitions except for the 397-keV transition where pure E2 was assumed. The proton branching ratios and β^+/EC intensities, calculated based on the total transition intensities, are indicated. In order to determine the branching ratios the absolute γ-ray efficiency of SeGA (see Sec. II) and the β and βp efficiencies of the DSSSD are needed which will be discussed in Sec. IV B and IV C. Furthermore, an accurate method of separating βp and β events is required. A Monte Carlo fitting procedure was developed based on the detector response to a known pure β emitter, ^{70}Br, which is covered in Sec. IV D. The derivation of the $\beta\gamma$ and βp branches shown in Fig. 8 are then discussed in Sec. IV E.

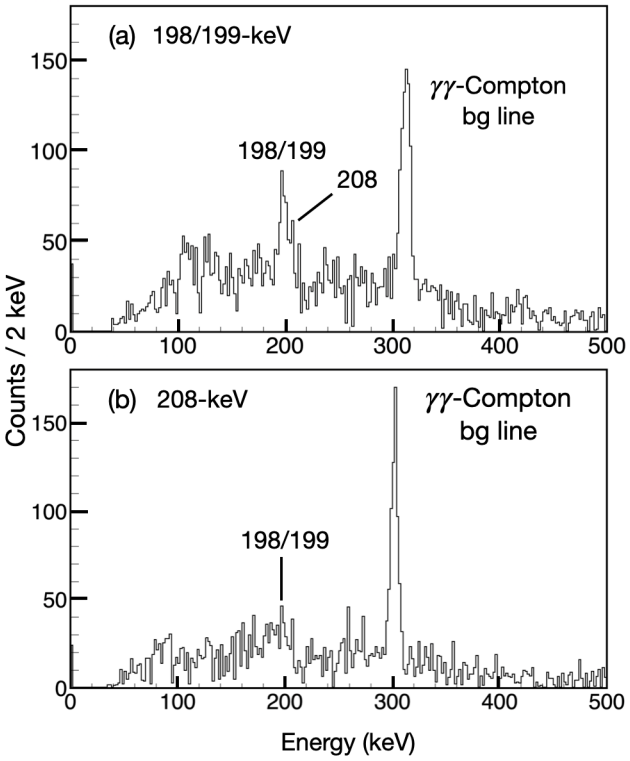

FIG. 5. Coincidence spectra used to determine γ-ray intensities and level feeding. Background-subtracted β-delayed $\gamma\gamma$ coincidence spectrum are shown gated on the (a) 198/199-keV and (b) 208-keV transitions. In (a) the 198/199-keV doublet peak shows self-coincidence and corresponds to feeding from the 407-keV state. A weak accumulation of counts centered around the 208-keV line is also observed. In (b) there is no significant indication of a 407-keV transition that would indicate feeding to the 615-keV state. In both spectra a peak originating from the projection of the intense 511-keV diagonal Compton band in the $\gamma\gamma$ coincidence matrix is observed.

B. DSSSD proton detection efficiency: ^{73}Sr experimental results

The proton detection efficiency of the DSSSD was measured using a known β-delayed proton emitter, ^{73}Sr, which is present in this data set. The Fermi β decay of the parent nucleus proceeds through the Isobaric Analog State (IAS) of the daughter nucleus ^{73}Rb and immediately proton decays to ^{72}Kr since even the ground state is significantly proton unbound. The total number of ^{73}Sr ions cleanly identified (i.e. an implantation pixel could be identified) was 3.6×10^2, and of these 3.3×10^2 were detected in time-correlation with an implant event, yielding a proton-detection efficiency of 90(7)%. As the efficiency is sensitive to the depth distribution of the implanted ions, LISE++ was used to verify that the average depth of both ^{73}Sr (235 μm) and ^{71}Kr (206 μm) was comparable.

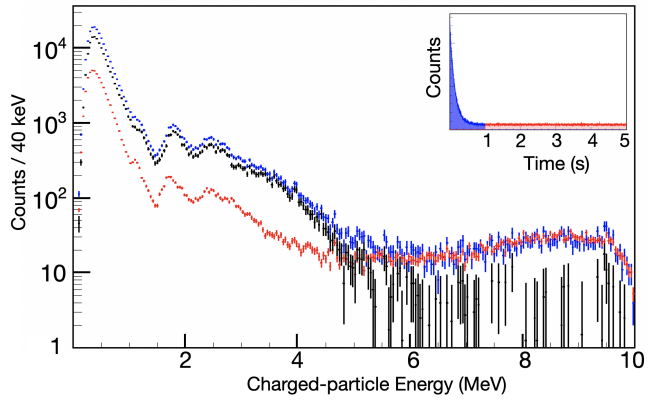

FIG. 6. Illustration of the component spectra and procedure used to obtain the ^{71}Kr background-subtracted charged-particle spectrum. Charged-particle spectra of decay events correlated within 1 s after implantation (blue) and a time normalized charged-particle spectrum of events correlated between 1-5 s after implantation (red) are shown. The inset shows a schematic representation of the events used in the background subtraction procedure. Residual (black) of the two spectra showing charged particles from ^{71}Kr β decay.

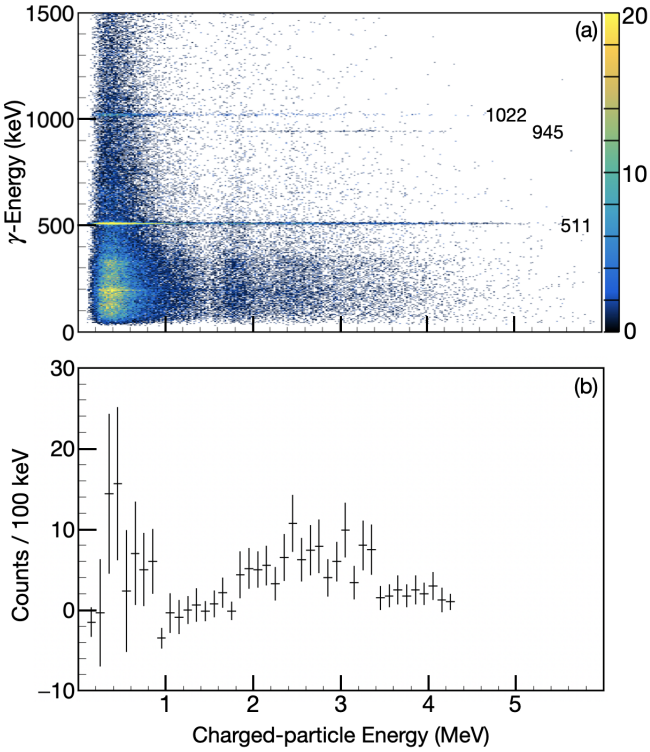

FIG. 7. Examination of charged particles coincident with γ rays following the decay of ^{71}Kr. Background-subtracted (a) γ-ray energy versus charged-particle energy matrix for ^{71}Kr β decay and (b) charged-particle energy spectrum in coincidence with 945-keV γ rays. The 945-keV γ ray is in coincidence with charged-particle energies from 1.5 to 5.0 MeV. The color scale represents the number of counts.

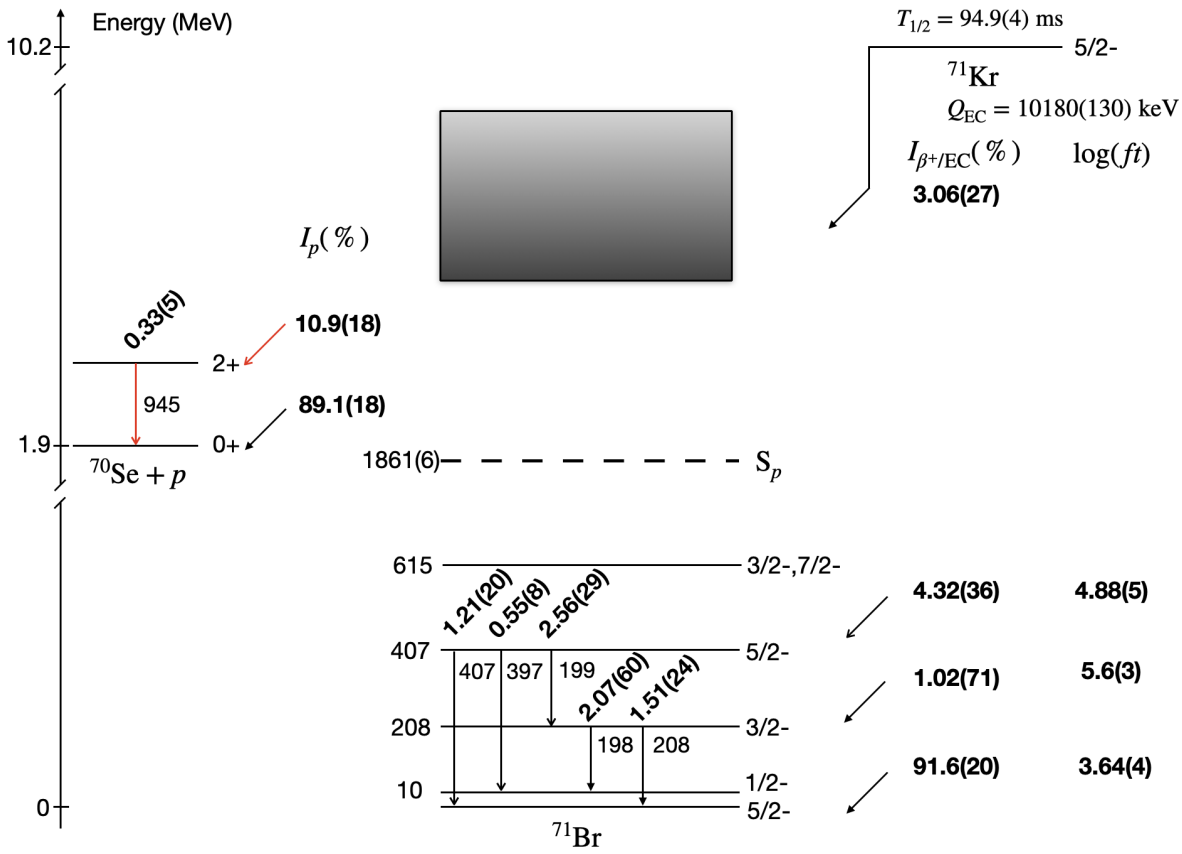

FIG. 8. Deduced β-delayed proton decay scheme of ^{71}Kr. Absolute intensities per 100 decays are given for the γ-ray transitions corrected for internal conversion, $I_{(\gamma+ce)}$, where the internal conversion coefficients were calculated using BrIcc assuming pure M1 transitions except for the 397-keV $5/2^- \rightarrow 1/2^-$ transition where pure E2 was assumed. Proton-unbound states (continuum of states) in ^{71}Br are denoted as a shaded rectangle. The newly observed feeding to the excited state in ^{70}Se in this experiment is shown in red (open arrow). Absolute β^+/EC intensities, $I_{\beta^+/EC}$, and log(ft) values should be taken as limits when considering possible unobserved feeding. If pure E2 transitions are assumed, the branching intensities to the 407-keV, 207-keV, and g.s. levels are 4.61(33)%, 0.77(74)%, and 91.6(20)%, respectively. Q_{EC} and S_p obtained from Ref. [30]

C. DSSSD β detection efficiency :^{70}Br experimental results

To calculate the β-detection efficiency and model the shape of the β spectrum in the charged-particle detector, a known almost pure β emitter, ^{70}Br, also in these data, was used. The 0^+ ground state and 9^+ isomer were both produced in the current study via the in-flight fragmentation of ^{92}Mo on a Be target. The half-lives extracted for the ground state of ^{70}Br and its 9^+ isomer are 79.1(6) ms and 2.3(5) s, respectively, as shown in Fig. 9. Due to the long-lived β-decaying isomer [31, 32], a time window from 20 s to 40 s was used for the background subtraction while events occurring within 20 s of implantation were considered. Production ratios of the ground state and 9^+ isomer were found to be 54(1)% and 46(2)%, respectively, as deduced from the decay-curve components. These half-lives are in good agreement with the ENSDF adopted values of $T_{1/2}(0^+) = 79.1(8)$ ms and $T_{1/2}(9^+) = 2.2(2)$ s [33] as well as the values 78.42(51) ms and 2157^{+53}_{-49} ms reported in a recent high-precision study [31]. We also note that we are in agreement with the result reported in Ref. [29] of 79.7(24) ms. The total number of ^{70}Br ions identified in the PID was 6.71×10^5, and of these 1.65×10^5 were detected in time-correlation as determined from the background subtracted decay curves. This analysis yielded a β-detection efficiency of 24.6(1)%, assuming a purely statistical error.

The validity of ^{70}Br being an almost pure β emitter is central to our analysis. The ^{70}Br ($T = 1$) ground state decays to ^{70}Se through a superallowed $0^+_{gs} \rightarrow 0^+_{gs}$ decay with a branching ratio of 97.94% and to the 2^+_1 with a 1.3% branch [31]. In contrast, the 9^+ ($T = 0$) isomer which has a Q_{EC} of 12.19 MeV for β decay, as determined using a total absorption spectrometer [31, 34], populates higher energy and higher spin states closer to the proton separation energy of 6.11 MeV in the ^{70}Se daughter. Feeding to states above the proton separation energy was not observed as evidenced by the comparison of the ^{70}Br charged-particle spectrum to that where a pure β-decay branch is isolated by using γ rays in the ^{70}Se daughter, as

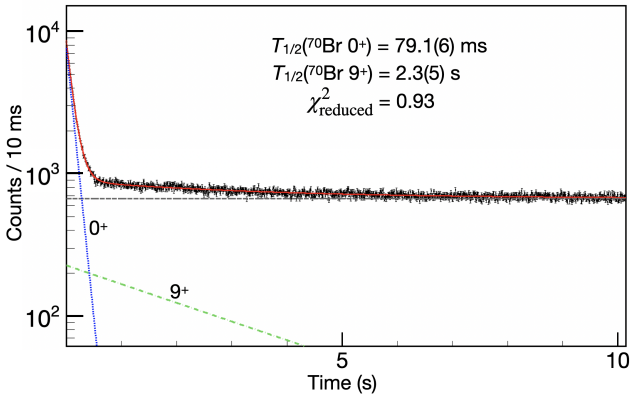

FIG. 9. Time distribution of decay events following the implantation of ^{70}Br nuclei. The spectrum was fit using exponential functions for the ^{70}Br ground state (blue) and 9^+ isomer (green) together with a constant background (gray), resulting in the combined fit (red). The half-lives extracted for the ^{70}Br ground state and 9^+ isomer are 79.1(6) ms and 2.3(5) s, respectively, where the uncertainty is composed of the statistical and systematic error added in quadrature.

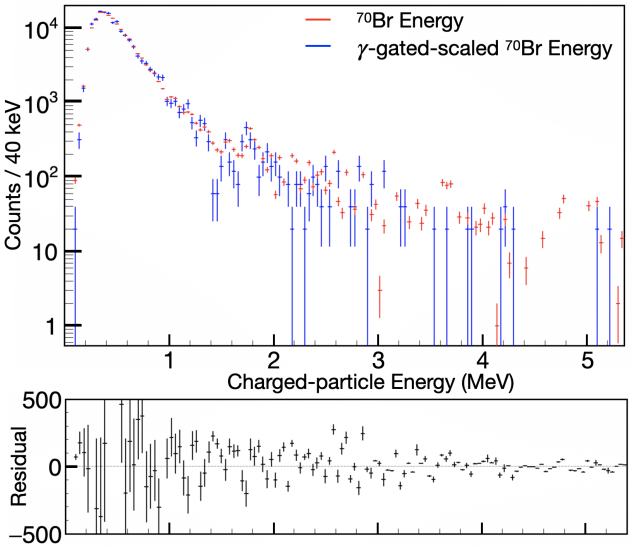

FIG. 10. Background subtracted charged-particle energy spectrum of (red) ^{70}Br and (blue) γ-gated (945, 964, and 1094 keV) β spectrum. The blue colored spectrum represents pure β decays of ^{70}Br due to the selection on ^{70}Se γ rays while the red spectrum could possibly contain proton decay events. The scaling factor was determined by minimizing the reduced χ^2 for energies below 1 MeV. The residual is presented in the bottom panel.

shown in Fig. 10. The origin of the feature near 1.8 MeV in this spectrum is unclear. It appears, however, in both the raw and ^{70}Se β-decay daughter γ-ray gated spectra, the latter of which should contain no βp events.

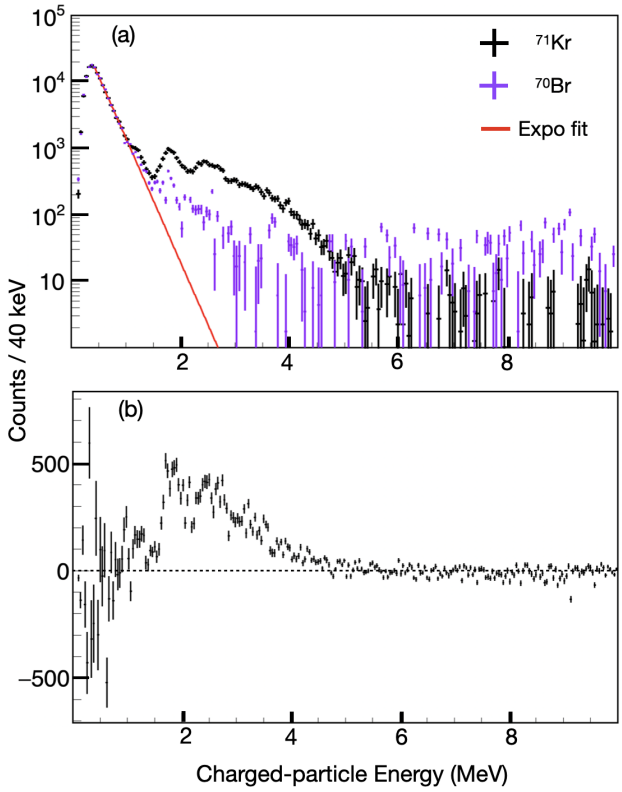

FIG. 11. Comparison of the exponential and Monte Carlo approach used to extract the number of emitted delayed protons. (a) ^{71}Kr background subtracted charged-particle energy spectrum (black). The results of two methods used to estimate the β spectrum are also shown: (red) An exponential fit of the low-energy β continuum and (purple) the ^{70}Br pure β charged-particle energy spectrum fit as described in the text. (b) A representative ^{71}Kr proton-energy spectrum obtained by subtracting the β background, modeled with the ^{70}Br method and mean scaling factor, from the measured ^{71}Kr spectrum.

D. Identification of proton events

As shown in Fig. 6, the decay-energy spectrum is continuous, and thus it is difficult to distinguish between the positrons expected at lower energies and the protons expected at higher energies on energy grounds alone. In order to quantitatively understand the charged-particle spectrum and to differentiate between positron and proton contributions, three different methods were investigated: a discrete energy cut, an exponential model of the β distribution, and a model of the detector response based on the essentially pure-β emitter, ^{70}Br.

The first method is a conventional one used in similar previous studies where a simple energy cut is defined, with the number of proton events being equal to the number of events above the chosen energy threshold [17, 29, 35, 36]. Using this method, we find the total number of protons to be $2.82(48)\times10^4$ by an integration from 1.1 to 10 MeV of the residual spectrum shown in

Fig. 6. The energy threshold of 1.1 MeV was chosen as this is approximately where the low energy β-dominated part of the spectrum begins to deviate from the expected shape of the β energy distribution. A similar choice was made in the previous studies, although slightly different energies were chosen depending mainly on the thickness of the DSSSD used. The systematic uncertainty was estimated by repeating the same procedure while changing the condition on the energy cut by $\pm$100 keV as was done in the previous studies using this method. The recorded uncertainty was obtained by adding the statistical and estimated systematic errors in quadrature.

A second method modeled the β distribution with an exponential function which is a better representation of the high-energy β tail compared to the energy cut method. This method was employed in a recent article by Orrigo et al. [37] which reported the results of an experiment with a similar detector setup and conducted at the RIKEN Nishina Center, where the decay of the neutron-deficient isotopes, ^{60}Ge and ^{62}Ge, were studied. In Fig. 11(a), the red line illustrates the exponential function fit to the data and following Orrigo et al. From this method we find the total number of protons is $2.47(11)\times10^4$ by an integration from 1.1 to 10.0 MeV of the spectrum shown in Fig. 11(b). The systematic uncertainty was estimated by repeating the exponential function fitting while changing the condition on the fit range by $\pm$100 keV. The recorded uncertainty was obtained by adding both the statistical and estimated systematic errors in quadrature.

A third approach was investigated in order to infer the true β-energy deposition in the DSSSD for the ^{71}Kr decay. Our method relies on using a pure β emitter in the data set, in our case ^{70}Br, as a template for the β energy distribution. As discussed, ^{70}Br has two β decaying states with transition energies which are close to the $Q_{\rm EC}$ value (10.2 MeV) of the decay of interest, ^{71}Kr. When the Q value is large enough the energy deposition of the β particles can be considered the same for both ions, as the stopping power in this energy region is fairly uniform [38]. Furthermore, simulations from LISE++ [39] show that the implantation depths for both species are approximately same, where an ion distribution centered in the DSSSD with a FWHM of 100 μm was found.

A Monte-Carlo approach was used to propagate statistical and systematic errors, where a set of pseudo charged-particle spectra for both ^{70}Br and ^{71}Kr were generated by randomly sampling the measured spectra using the statistical error in the measurement. For each generated pseudo spectrum, an upper fit range was also randomly selected from a Gaussian centered at 1100-keV with σ = 250 keV in order to incorporate systematic effects on the choice of fitting range. The distribution of ^{70}Br events was then fit with a scaling factor to the ^{71}Kr spectrum using the chosen fitting range. The number of protons was then inferred by integrating the full residual spectrum.

The ensemble of scale factors and fitting ranges both follow a Gaussian frequency distribution, where the mean values of these distributions were used to select representative best-fit values. These values were then used to generate the representative spectrum for ^{70}Br shown in Fig. 11(a). In the subtracted spectrum shown in Fig. 11(b), there is a broad distribution of protons from 1.5 to 5.0 MeV. At low energies the uncertainty of the background subtraction is rather large and there does not appear to be a statistically significant number of observed protons. However, as shown in Fig. 7(b), there do appear to be a significant number of low-energy protons associated with the 945-keV γ-ray transition. This observation suggests there are proton-unbound levels close in relative energy to the 945-keV 2^+ state of ^{70}Se with the emitted protons depositing energies around 0.5 MeV. Furthermore the proton spectrum represents qualitatively, the convolution of the level density of proton fed states in the compound nucleus and the β-strength function. Using the Monte-Carlo procedure, the distribution of proton events identified is represented by the value $1.91(8)\times10^4$ protons.

TABLE I. Proton branching ratio calculated by the three different methods discussed in the text.

Method	Proton Count	Proton branching ratio(%)
Energy cut	$2.82(48)\times10^4$	4.5(8)
Exponential fitting	$2.47(11)\times10^4$	4.0(4)
Monte-Carlo fitting procedure	$1.91(8)\times10^4$	3.06(27)

The exponential-function fitting method, and the method outlined here using an implanted pure-β emitter, model the higher energy β distribution/tail differently. Our results show that the long-tail from the Landau distribution of β-particle deposition energies extends well into the region of proton events, as compared in Fig. 11(a). By characterizing the tail of the β-particle energy deposition with an exponential the resulting number of protons will be significantly overestimated and thus the overall proton branching, which is exacerbated even more with a simple energy cut. The progression of numbers in Table I given by different methods, confirms the overestimation of the proton branching ratio when not accounting for the long-tail from the Landau distribution of β-particle energy depositions. As one can see, the energy-cut method is consistent with the results first reported by Blank et al. [17], but the proton branching obtained by the new approach is in agreement with results reported by Oinonen et al. [18] which had a proper method to distinguish β's and protons by using a detection setup that consisted of a ΔE-E telescope. Furthermore, the outlined method accounts for the systematic error of the experimental setup more realistically, while also incorporating any statistical effects on the total number of

protons measured.

The most salient feature in the residual ^{71}Kr β-delayed proton spectrum (Fig. 11) is a peak near 1.8 MeV in energy. This peak is distinct in the residual delayed proton spectrum of Fig. 6 but absent from the 945-keV γ-gated spectrum in Fig. 7(b). Together, this suggests a state, or close group of states at about 3.6 MeV in excitation in ^{71}Br which are well populated in the β decay and which directly decay to the ^{70}Se ground state. A candidate for this level, or levels, is the $T = 3/2$ Isobaric Analog State (IAS). Using the accurately known mass of ^{71}Se and the Isotopic Multiplet Mass Equation (IMME) estimates can be made for the location of this level in ^{71}Br. If the 2013 compilation of Mass Multiplets is used [40] an excitation of 3.2 MeV would be inferred, but a more recent fit to masses in this region [41] suggest a higher excitation, nearer to $\approx$ 3.6 MeV, and very close to the observed peak.

E. Determination of $\beta\gamma$ and βp branches

The technique used in this current study involved the direct identification and counting of cleanly identified (see Fig. 3) implanted ions at a rate of $\approx$ 10 ions/sec, so pile-up and dead time losses were small, and the source strength was known absolutely. There were $6.930(8)\times10^5$ identified ^{71}Kr ions in this counting sample. This facilitates determination of the absolute branching ratios to both the ground state and excited states. It has less systematic uncertainty than the more commonly used decay counting approach which must be used when the source strength is not known, but which is more sensitive to systematic uncertainty in the absolute response of the detectors. In this work we use the source strength as our primary normalization.

For consistency, the number of identified ^{71}Kr implants was compared to the number of spatially correlated decays. Using the efficiencies discussed in the preceding sections (90(7)% for protons and 24.6(1)% for positrons) we reconstruct only 89% of the decays. This shortfall mainly arises from uncertainty in the positron detection efficiency. The physical topology of ^{70}Br implanted ions on the decay DSSSD, used for the determination of positron efficiency, was slightly different from the ^{71}Kr ions, and edge effects and small corrections for dead strips might cause the positron efficiency to change slightly. For example, the number of implanted ions would exactly match the number of decays if the positron efficiency was about 11% lower at 21.8%. In all, the absolute normalization of decay branches to the number of implanted ions appears to be most reliable, and so this is the value used to calculate the absolute intensities shown in Table II. However, in order to reconcile this discrepancy an estimated 10% systematic error was included into the β efficiency when determining the uncertainty on the reported values.

For each of the five identified γ-ray lines the absolute intensities per 100 decays was found, utilizing the γ-ray, β, and βp efficiencies determined for the detector suite. These numbers are to be contrasted with relative intensities found by Oinonen et al. where the relative intensity between the 208- and 198-keV γ-ray lines found previously, 0.36, is consistent within 1σ of our values. Utilizing these absolute intensities and the coincidence data, the level scheme in Fig. 8 was then constructed assuming that there was no population of the 615-keV state in ^{71}Br.

The branch to proton unbound states is most straightforward. Using the Monte Carlo decomposition discussed in Sec. IV D and the proton efficiency from Sec. IV B we determine there were $2.2(2)\times10^4$ correctly correlated protons. Thus, the β-delayed proton branch is 3.06(27)%. The difference compared to previous studies is due to our more refined Monte-Carlo decomposition of the charged particle spectrum into positrons and protons.

A key new observation in this work was finding significant population of the first excited state of the βp daughter, ^{70}Se, through the detection of the 945-keV decay γ ray. A search of other known transitions in ^{70}Se was inconclusive. With the known efficiency of SeGA (Sec. II) an excited-state branch of 10.9(18)% was extracted. This observation is important in constraining the spin of ^{71}Kr as is discussed below.

The branches to excited states in ^{71}Br could be determined in a similar fashion. A search was made for population of other known levels, but only clear evidence was found for population for the 208- and 407-keV states as there was no notable signal of a coincidence between 407- and 208-keV γ rays. Branches of 4.32(36)% and 1.02(71)% were inferred for the 407- and 208-keV levels, respectively. The remaining strength is assumed to be in decays to the ground state. The ground-state branch is found to be 91.6(20)%.

A comparison with the previously measured [17, 18] and deduced [20] branching ratios is shown in Table III. The current results are not in complete agreement with previous measurements. The branching to the 208-keV state of 1.02(71)% is significantly different from the previous observation of 15.8(14)% due to the association of 208-keV γ rays fed from the 407-keV state in ^{71}Br as the 4.32(36)% branch feeding we found to the 407-keV state was not observed by Oinonen et al. [18]. The feeding inferred by Fischer et al. [20] was based on measuring many new transitions in ^{71}Br and analyzing some of the corresponding peaks in Oinonen's published spectrum. However, Fischer et al. interpreted their findings as showing even more strength to excited states, and consequently inferred less to the ground state. In fact, the current data show that the new peaks just represent a redistribution of decay strength amongst excited states, without significantly altering the ground-state branch. Thus, the anomalously strong β decay (15% each) to excited states suggested by Fischer et al. may have come from mis-normalization and is not supported by this work.

TABLE II. Absolute intensities per 100 decays for the five γ-ray lines observed in the β decay of ^{71}Kr. Intensities in this table do not account for internal conversion.

E_γ (keV)	198/199[a]	208.0(2)	397.1(3)	407.4(4)	943.7(5)
I_γ (%)	4.54(51)	1.48(23)	0.55(8)	1.21(20)	0.33(5)
$N_{\beta\gamma}$	1490(75)	477(58)	117(11)	256(32)	144(16)
N_β	$6.930(8)\times10^5$				
ϵ_γ	0.1926(30)	0.1885(30)	0.1267(42)	0.1242(42)	0.0695(36)
ϵ_β	0.246(25)[b]	0.246(25)	0.246(25)	0.246(25)	0.90(7)

[a] Individual 198- and 199-keV energies are considered degenerate in this work and could not be resolved. An intensity for the doublet is given where the 198/199-keV peak is observed at 198.3(2) keV.
[b] Includes the estimated 10% systematic error.

TABLE III. β and βp branching ratio obtained for ^{71}Kr in the present work compared to literature values.

Energy (keV)	I (%) [17]	I (%) [18]	I (%) [20][a]	I (%) This study
β branching ratios				
g.s	-	82.1(16)	68	91.6(20)
208	-	15.8(14)	15	1.02(71)
407	-	-	15	4.32(36)
unbound continuum	5.2(6)	2.1(7)	2	3.06(27)
proton branching ratios				
g.s	-	-	-	89.1(18)
945	-	-	-	10.9(18)

[a] Not obtained by a direct β-decay measurement. Deduced by analyzing branching ratios from [18].

V. DISCUSSION AND CONCLUSION

In a world where isospin symmetry is exact, the β decay between a $T = 1/2$ mirror pair represents the simplest transformation of a proton to a neutron with no change in the spatial or spin wave functions. The matrix element is simply the isospin lowering operator, τ. The decay should be very fast, dictated by the weak coupling constants and the Q value. If the symmetry is perfect the decay would be purely ground state-to-ground state. Deviation from this ideal reflects the degree of broken symmetry.

The central goal of this work was to determine whether the nuclide ^{71}Kr and its mirror partner ^{71}Br have the same ground-state spin and parity, namely $J^\pi = 5/2^-$. It has been suggested [19] that the ground state of ^{71}Kr was interchanged with the closely spaced first-excited state. This is plausible; isospin symmetry breaking has recently been observed in the $A = 73$ mirror pair, where the ground-state spins of ^{73}Sr and ^{73}Rb differ [42] due to an inversion of states that are only 27-keV apart. In the case of ^{71}Br, there is only a 10-keV separation between the ground and first-excited states.

To address this question, the β-decay branches of ^{71}Kr were measured absolutely in order to constrain the ground-state spin of ^{71}Kr. Specifically, a signature of the population to $7/2^-$ states of ^{71}Br were searched for as this would rigorously preclude a low-spin parent. These states were not observed. However, the large branching to excited states inferred in [20] appear incorrect, and we now measure smaller branches, consistent with other $T = 1/2$ mirror pairs. The fact that the $J^\pi = 5/2^-$ state at 407 keV is populated at the 4% level indicates that symmetry-breaking effects, mostly Coulomb, do distort the known shape co-existence and perfect mirror symmetry is broken but not sufficiently to make parent and daughter spins differ.

Precise knowledge of the ^{71}Kr half-life, as well as other $T = 1/2$ nuclear mirror transitions, is an important input for tests of the electroweak standard model and determining the V_{ud} quark-mixing element of the Cabibbo-Kobayashi-Maskawa (CKM) matrix [7, 43]. The significant disagreement with both Ref. [18] and Ref. [29], therefore, requires a careful discussion. In Ref. [18] both protons and positrons were uniquely identified and their energies measured. This allowed the half-life to be determined using two methods; one relied on constructing a decay curve using only proton events while the other method used only high-energy (> 5.5 MeV) β's thereby yielding half-lives of 95(6) ms and 101(4) ms, respectively. The ENSDF value of 100(3) ms is the weighted average reported in Ref. [18]. If these measurements are considered independently, the half-life as determined using protons is in agreement with our result while that determined using high-energy β's is in disagreement, suggesting an unaccounted systematic effect. The experiment in Ref. [29] was performed at RIKEN and used an implantation setup and techniques similar to the present experiment. A half-life with similar precision is reported yet the values disagree by almost 10σ. This could be due to differing background contaminants in the beams from each experiment. We note, however, that our current result is based on significantly more ^{71}Kr implants by nearly a factor of 40, so it is difficult to reconcile the fact that the levels of precision are reported to be similar.

The combination of absolute ^{71}Kr ion counting and

the determination of true implant-β, implant-$\beta\gamma$ and implant-βp coincident intensities allow the absolute β-transition rates to be extracted with a technique that is complementary to previous determinations. With the new half-life of 94.9(4) ms, a ground-state branch of 91.6(20)%, and the latest mass data [44], a $\log(ft) = 3.64(4)$ was determined for the ^{71}Kr to ^{71}Br ground state-to-ground state decay. Surveying the known lighter 26 $T = 1/2$ mirror pairs [7, 44, 45], all of which have the same spin and parity for parent and daughter, this is very close to the mean value. Excepting the cases immediately adjacent to shell closures at ^{16}O and ^{40}Ca, 17 of 20 decays have $\log(ft)$ values between 3.6 and 3.7, that is having ft values 4000-5000. The lighter cases have 99% ground state-to-ground state decay branches which falls to $\approx$ 90% in the heavier systems presumably due to increased Coulomb distortion. In all of the well-studied cases the $\log(ft)$ values to excited states are substantially larger, with $\log(ft)$ >4.3 (ie ft values >20,000) even when they have the same spin and parity as the ground state. In the current ^{71}Kr to ^{71}Br case the decay to the $J^\pi = 3/2^-$ 208-keV state has $\log(ft)$ >5.6 and to the $J^\pi = 5/2^-$ 407-keV state $\log(ft)$ >4.88. For the excited states only a limit can be set on the $\log(ft)$ values as unseen population from higher lying states cannot be excluded. Nonetheless, all these decay rates are consistent with the ground state of ^{71}Br being the true mirror of ^{71}Kr and both having $J^\pi = 5/2^-$.

The observed features of the β-delayed proton energy spectrum obtained for ^{71}Kr confirm that a continuum of proton decaying states in ^{71}Br are being populated by the β decay of ^{71}Kr, as was previously reported [18]. β-delayed proton emission provides another method of probing the spin of decaying states, as the proton decay is sensitive to the tunneling of the proton, so is sensitive to the orbital angular momentum of the decay [46]. Specifically, the observation of a proton-decay branch to the 2^+ state in ^{70}Se strengthens the idea that the ground state of ^{71}Kr is $J^\pi = 5/2^-$ [47–49]. For there to be an appreciable decay branch to the $J^\pi = 2^+$ state in ^{70}Se, the initial unbound states in ^{71}Br must have $J \geq 5/2$. If the ground state of ^{71}Kr were to have $J^\pi = 1/2^-$ spin then this would be inhibited, involving forbidden β decay and the β-delayed proton decay would be almost exclusively to the ^{70}Se ground state. The 3.06(27)% of the β decay that proceeds to proton unbound states must also be very fast to compete, despite restricted phase space. If all the proton-unbound decay proceeded to a single state, the equivalent $\log(ft)$ value would be 4.10(7), as might be expected for a decay to the $T = 3/2$ Isobaric Analog State which would also have $J^\pi = 5/2^-$. In fact, the delayed proton spectrum is very extended as the β decay to unbound states is to a broad domain from 2-7 MeV in excitation in ^{71}Br but which includes a peak of substantial strength at 1.8 MeV, suggesting a state corresponding to $\approx$ 3.6 MeV excitation, where the lowest $T = 3/2$ state is anticipated.

ACKNOWLEDGMENTS

We would like to thank T. Ginter for his effort in providing the ^{73}Sr beam used in the experiment. We acknowledge support from the US DOE, Office of Science, Office of Nuclear Physics under award numbers DE-FG02-94ER40848 (UML), DE-AC02-06CH11357 (ANL), as well as DE-FG02-88ER40387 and DE-SC0019042 (OU); the NNSA through award numbers DE-NA0003180 (NSSC), DE-NA0000979 (NSSC), DE-NA0003221, DE-NA0003909 and/or DE-NA0002132; and the NSF under contract numbers PHY-1-102511 and PHY 14-30152. This work was performed under the auspices of the U.S. Department of Energy by Lawrence Livermore National Laboratory under Contract DE-AC52-07NA27344.

[1] W. Heisenberg, Zeitschrift für Physik **77**, 1 (1932).
[2] J. P. Elliott and P. G. Dawber, Symmetry in Physics. Vol. 1: Principles And Simple Applications (MacMillan Press Limited, 1987).
[3] D. D. Warner, M. A. Bentley, and P. V. Isacker, Nature Phys. **2**, 311 (2006).
[4] P. Bączyk, J. Dobaczewski, M. Konieczka, W. Satuła, T. Nakatsukasa, and K. Sato, Phys. Lett. B **778**, 178 (2018).
[5] E. Wigner, Phys. Rev. **51**, 106 (1937).
[6] A. A. Frank, Symmetry in Physics: Principles And Simple Applications, 1st ed., Vol. 230 (Springer, 2009).
[7] N. Severijns, M. Tandecki, T. Phalet, and I. S. Towner, Phys. Rev. C **78**, 055501 (2008).
[8] J. H. Hamilton, A. V. Ramayya, W. T. Pinkston, R. M. Ronningen, G. Garcia-Bermudez, H. K. Carter, R. L. Robinson, H. J. Kim, and R. O. Sayer, Phys. Rev. Lett. **32**, 239 (1974).
[9] B. Varley, M. Campbell, A. Chishti, W. Gelletly, L. Goettig, C. Lister, A. James, and O. Skeppstedt, Phys. Lett. B **194**, 463 (1987).
[10] A. Gade, D. Bazin, A. Becerril, C. M. Campbell, J. M. Cook, D. J. Dean, D. C. Dinca, T. Glasmacher, G. W. Hitt, M. E. Howard, *et al.*, Phys. Rev. Lett. **95**, 022502 (2005).
[11] T. R. Rodríguez, Phys. Rev. C **90**, 034306 (2014).
[12] P. Möller, A. Sierk, T. Ichikawa, and H. Sagawa, Atomic Data and Nuclear Data Tables **109-110**, 1 (2016).
[13] K. Wimmer, W. Korten, T. Arici, P. Doornenbal, P. Aguilera, A. Algora, T. Ando, H. Baba, B. Blank, A. Boso, *et al.*, Phys. Lett. B **785**, 441 (2018).
[14] K. Wimmer, W. Korten, P. Doornenbal, T. Arici, P. Aguilera, A. Algora, T. Ando, H. Baba, B. Blank, A. Boso, *et al.*, Phys. Rev. Lett. **126**, 072501 (2021).
[15] G. Flerov, V. Karnaukhov, G. Ter-Akopyan, L. Petrov, and V. Subbotin, Nucl. Phys. **60**, 129 (1964).
[16] G. Ewan, E. Hagberg, P. Hansen, B. Jonson, S. Mattsson, H. Ravn, and P. Tidemand-Petersson, Nucl. Phys. A **352**,

13 (1981).
[17] B. Blank, S. Andriamonje, S.and Czajkowski, F. Davi, R. Del Moral, C. Donzaud, J. Dufour, A. Fleury, A. Grewe, R. Grzywacz, *et al.*, Phys. Lett. B **364**, 8 (1995).
[18] M. Oinonen, A. Jokinen, J. Äystö, P. Baumann, F. Didierjean, A. Honkanen, A. Huck, M. Huyse, A. Knipper, G. Marguier, *et al.*, Phys. Rev. C **56**, 745 (1997).
[19] P. Urkedal and I. Hamamoto, Phys. Rev. C **58**, R1889 (1998).
[20] S. M. Fischer, T. Anderson, P. Kerns, G. Mesoloras, D. Svelnys, C. J. Lister, D. P. Balamuth, P. A. Hausladen, and D. G. Sarantites, Phys. Rev. C **72**, 024321 (2005).
[21] D. Morrissey, B. Sherrill, M. Steiner, A. Stolz, and I. Wiedenhoever, Nucl. Instrum. Methods B: **204**, 90 (2003).
[22] D. Bazin, V. Andreev, A. Becerril, M. Doléans, P. Mantica, J. Ottarson, H. Schatz, J. Stoker, and J. Vincent, Nucl. Instrum. Methods A **606**, 314 (2009).
[23] J. Prisciandaro, A. Morton, and P. Mantica, Nucl. Instrum. Methods A **505**, 140 (2003).
[24] W. Mueller, J. Church, T. Glasmacher, D. Gutknecht, G. Hackman, P. Hansen, Z. Hu, K. Miller, and P. Quirin, Nucl. Instrum. Methods A: **466**, 492 (2001).
[25] C. J. Prokop, S. N. Liddick, B. Abromeit, A. T. Chemey, N. Larson, S. Suchyta, and J. R. Tompkins, Nucl. Instrum. Methods A **741**, 163 (2014).
[26] E. Hagberg, J. Hardy, H. Schmeing, H. Evans, U. Schrewe, V. Koslowsky, K. Sharma, and E. Clifford, Nucl. Phys. A **383**, 109 (1982).
[27] B. O. ten Brink, R. D. Vis, A. W. B. Kalshoven, and H. Verheul, Zeitschrift für Physik **270**, 83 (1974).
[28] G. Gürdal and E. A. McCutchan, Nuclear Data Sheets for A = 70, Nucl. Data Sheets **136**, 1 (2016).
[29] L. Sinclair, R. Wadsworth, J. Dobaczewski, A. Pastore, G. Lorusso, H. Suzuki, D. S. Ahn, H. Baba, F. Browne, P. J. Davies, *et al.*, Phys. Rev. C **100**, 044311 (2019).
[30] M. Wang, G. Audi, F. G. Kondev, W. Huang, S. Naimi, and X. Xu, The AME2016 atomic mass evaluation (II). tables, graphs and references, Chinese Physics C **41**, 030003 (2017).
[31] A. I. Morales, A. Algora, B. Rubio, K. Kaneko, S. Nishimura, P. Aguilera, S. E. A. Orrigo, F. Molina, G. de Angelis, F. Recchia, *et al.*, Phys. Rev. C **95**, 064327 (2017).
[32] A. Vitéz-Sveiczer, A. Algora, A. Morales, B. Rubio, G. Kiss, G. de Angelis, F. Recchia, S. Nishimura, J. Agramunt, V. Guadilla, *et al.*, Acta Phys. Polon. B **51**, 587 (2020).
[33] G. Gürdal and E. A. McCutchan, Nuclear Data Sheets **136**, 1 (2016).
[34] M. Karny, L. Batist, D. Jenkins, M. Kavatsyuk, O. Kavatsyuk, R. Kirchner, A. Korgul, E. Roeckl, and J. Żylicz, Phys. Rev. C **70**, 014310 (2004).
[35] C. Dossat, N. Adimi, F. Aksouh, F. Becker, A. Bey, B. Blank, C. Borcea, R. Borcea, A. Boston, M. Caamano, *et al.*, Nucl. Phys. A **792**, 18 (2007).
[36] S. E. A. Orrigo, B. Rubio, Y. Fujita, B. Blank, W. Gelletly, J. Agramunt, A. Algora, P. Ascher, B. Bilgier, L. Cáceres, *et al.*, Phys. Rev. Lett. **112**, 222501 (2014).
[37] S. E. A. Orrigo, B. Rubio, W. Gelletly, P. Aguilera, A. Algora, A. I. Morales, J. Agramunt, D. S. Ahn, P. Ascher, B. Blank, *et al.*, Phys. Rev. C **103**, 014324 (2021).
[38] Z. Meisel, M. Santo, H. Crawford, R. Cyburt, G. Grinyer, C. Langer, F. Montes, H. Schatz, and K. Smith, Nucl. Instrum. Methods A **844** (2016).
[39] O. Tarasov *et al.*, Nucl. Instrum. Methods B: **266**, 4657 (2008).
[40] Y. H. Lam, B. Blank, N. A. Smirnova, J. B. Bueb, and M. S. Antony, Atomic Data and Nuclear Data Tables **99**, 680 (2013).
[41] D. E. M. Hoff, A. M. Rogers, Z. Meisel, P. C. Bender, K. Brandenburg, K. Childers, J. A. Clark, A. C. Dombos, E. R. Doucet, S. Jin, *et al.*, Phys. Rev. C **102**, 045810 (2020).
[42] D. E. M. Hoff, A. M. Rogers, S. M. Wang, P. C. Bender, K. Brandenburg, K. Childers, J. A. Clark, A. C. Dombos, E. R. Doucet, S. Jin, *et al.*, Nature **580** (2020).
[43] O. Naviliat-Cuncic and N. Severijns, Phys. Rev. Lett. **102**, 142302 (2009).
[44] M. Wang, W. Huang, F. Kondev, G. Audi, and S. Naimi, Chinese Phys. C **45**, 030003 (2021).
[45] ENSDF, `https://www.nndc.bnl.gov` (2022).
[46] M. Karny, K. Rykaczewski, R. Grzywacz, J. Batchelder, C. Bingham, C. Goodin, C. Gross, J. Hamilton, A. Korgul, W. Królas, *et al.*, Phys. Lett. B **664**, 52 (2008).
[47] A. M. Rogers, M. A. Famiano, W. G. Lynch, M. S. Wallace, F. Amorini, D. Bazin, R. J. Charity, F. Delaunay, R. T. de Souza, J. Elson, *et al.*, Phys. Rev. Lett. **106**, 252503 (2011).
[48] A. M. Rogers, J. Giovinazzo, C. J. Lister, B. Blank, G. Canchel, J. A. Clark, G. de France, S. Grévy, S. Gros, E. A. McCutchan, *et al.*, Phys. Rev. C **84**, 051306(R) (2011).
[49] M. Del Santo, Z. Meisel, D. Bazin, A. Becerril, B. Brown, H. Crawford, R. Cyburt, S. George, G. Grinyer, G. Lorusso, *et al.*, Phys. Lett. B **738**, 453 (2014).